Radical Chemistry

DOI: 10.1002/anie.201302506

Single and Double N–H Bond Activation of Ammonia by $[Al_2O_3]^{\bullet+}$: Room Temperature Formation of the Aminyl Radical and Nitrene**

*Robert Kretschmer, Zhe-Chen Wang, Maria Schlangen, and Helmut Schwarz**

Dedicated to the Bayer company on the occasion of its 150th anniversary

As nitrogen-containing compounds occupy a central role in chemistry, improving the repertoire of methods to form C–N bonds constitutes an important, ongoing issue.[1] Unfortunately, "classical methods" for the generation of nitrogen-containing compounds require a pre-functionalization of the substrates, thus causing an increased synthetic complexity.[2] Consequently, catalytic direct C–H amination reactions represent a formidable challenge,[3] and the development or improvement of C–N coupling methods employing NH_3 are, because of its low price and the nearly unlimited availability, of particular interest.[3d] Although the activation of N–H bonds corresponds to the key step in the derivatization of amines and ammonia, there is only limited knowledge about the elementary steps involved in the N–H bond activation in solution.[3c,4] In contrast, quite a few gas-phase experiments, which provide an ideal arena for probing mechanistic features of a chemical process at a strictly molecular level,[5] have been performed to address various aspects of C–H[6] and N–H bond-activation processes.[7] In particular, cationic metal oxides as well as oxo clusters have been found to be versatile reagents for the activation of C–H bonds.[6a,b,8] Despite promising results, related studies about the activation of ammonia mediated by metal oxides and metal oxide clusters are relatively scarce.[7b,d,9] Among them, systematic investigations have revealed that cationic first-row transition-metal oxides $[MO]^+$ (Sc–Ni, Zn) react with ammonia mainly under water elimination or hydrogen-atom transfer (HAT) [Eq. (1) and (2)].[7d,9a,b,e] HAT was also observed for the alkaline-earth-metal oxides $[CaO]^+$, $[BaO]^+$, and $[SrO]^+$.[7b]

$$[MO]^+ + NH_3 \rightarrow [M(NH)]^+ + H_2O \quad (1)$$

$$[MO]^+ + NH_3 \rightarrow [M(OH)]^+ + NH_2^{\bullet} \quad (2)$$

In addition, the reactivity of transition-metal oxide cluster ions with NH_3 has been studied in quite some detail: Although $[OsO_3]^+$,[9c] $[MoO_m]^+$ $(m = 1–3)$,[9d] and $[Mn_2O_2]^+$[9f] are not reactive, clusters such as $[Co_nO_m]^+$ and $[Fe_nO_m]^+$ $(n = 3–6,\ m = 0–3)$ react with ammonia in a size-dependent fashion under 1) adduct formation $[M_nO_m(NH_3)]^+$, 2) atomic metal release to produce $[M_{n-1}O_m(NH_3)]^+/M$, and 3) dehydrogenation to form $[M_nO_m(NH)]^+/H_2$.[9g] In the context of catalytic reduction of nitric oxides by ammonia, multi-collision experiments of neutral vanadium oxide clusters with mixtures of NO and NH_3 revealed that both N_2 and H_2O are generated.[10] Further, dehydration is observed when NH_3 reacts with $[OsO_m]^+$ $(m = 1,2)$,[9c] and $[Mo_3O_9]^+$[9d] whereas $[OsO_4]^+$ brings about HAT.[9c] Cationic aluminum oxide clusters are of special interest[11] because γ-Al_2O_3 is broadly used as a catalyst or catalyst support in many industrial applications.[12] Several $[(Al_2O_3)_x]^{\bullet+}$ species $(x = 1,$ 3–5) bring about HAT in their thermal reactions with methane [Eq. (3)];[11b,13] moreover, $[Al_2O_3]^{\bullet+}$ shows another

$$[(Al_2O_3)_x]^{\bullet+} + CH_4 \rightarrow [(Al_2O_3)_xH]^+ + CH_3^{\bullet} \quad (3)$$

remarkable reactivity, that is, the generation of $[Al_2O_2H_2]^{\bullet+}$ by liberation of neutral formaldehyde [Eq. (4)].[11b] Regarding

$$[Al_2O_3]^{\bullet+} + CH_4 \rightarrow [Al_2O_2H_2]^{\bullet+} + CH_2O \quad (4)$$

the desired activation of ammonia, $[Al_2O_3]^{\bullet+}$ combines two interesting features: 1) the spin density is located at the terminal oxygen atom and is thus beneficial for a HAT process,[6c,11b] and 2) the two aluminum centers in $[Al_2O_3]^{\bullet+}$ can act as a Lewis acid and can thus attract the nitrogen lone-pair of NH_3. Further, high catalytic activities are observed, when Al_2O_3 is used as a support for the decomposition of ammonia,[14] which may be important in the context of hydrogen generation for fuel cells.[15] These findings raise the question of the active site of the catalysts and the mechanistic aspects of N–H bond activation by aluminum oxide. Thus, we investigated the reactivity of $[Al_2O_3]^{\bullet+}$ towards NH_3 in a combined experimental/computational study.

Figure 1 a,b show the thermal reactions of mass-selected $[Al_2O_3]^{\bullet+}$ ions with NH_3 and ND_3, respectively. As observed

[*] Dr. R. Kretschmer, Dr. Z.-C. Wang, Dr. M. Schlangen, Prof. Dr. H. Schwarz
Institut für Chemie, Technische Universität Berlin
Strasse des 17. Juni 135, 10623 Berlin (Germany)
E-mail: Helmut.Schwarz@tu-berlin.de
Dr. R. Kretschmer
University of California, San Diego
Department of Chemistry and Biochemistry (USA)
Dr. Z.-C. Wang
Colorado State University, Department of Chemistry (USA)

[**] Financial support from the Fonds der Chemischen Industrie and the Cluster of Excellence "Unifying Concepts in Catalysis" (EXC 314/1) funded by the Deutsche Forschungsgemeinschaft and administered by the Technische Universität Berlin is gratefully acknowledged. R.K. acknowledges the Stiftung Stipendien Fonds des Verbandes der Chemischen Industrie for a Kekulé scholarship and the Alexander von Humboldt-Stiftung (AvH) for a Feodor Lynen Research Fellowship. Z.-C.W. is grateful for an AvH Fellowship. We thank Dr. Thomas Weiske for enlightening discussions and the Institut für Mathematik der TU Berlin for the allocation of computer time.

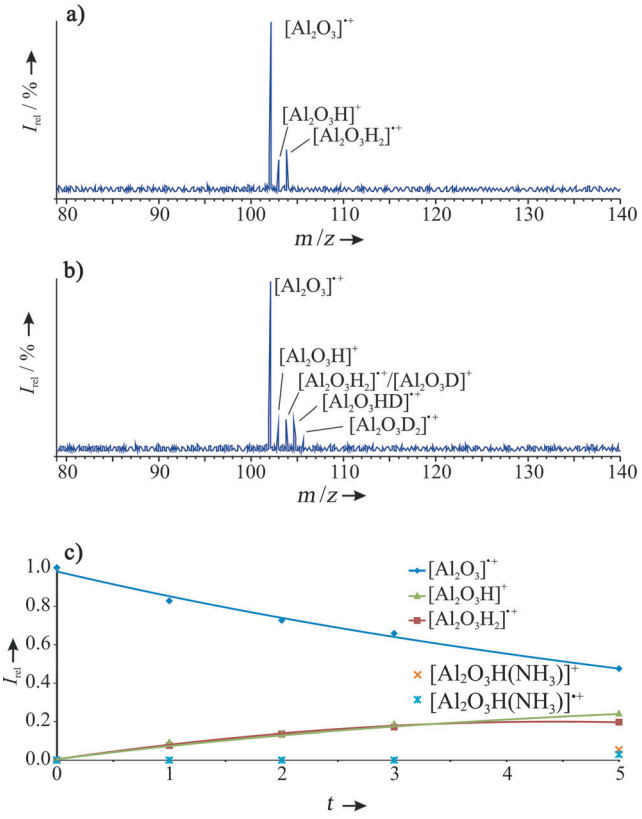

Figure 1. Ion–molecule reactions of mass-selected $[Al_2O_3]^{\bullet+}$ clusters with a) NH_3 ($p = 3.5 \times 10^{-9}$ mbar), and b) ND_3 ($p = 4.3 \times 10^{-9}$ mbar) at a reaction delay of 3 s; c) intensity profile of the parent and product ions as a function of time for the reaction with NH_3.

earlier for the $[Al_2O_3]^{\bullet+}/CH_4$ couple,[11b] HAT takes place resulting in the formation of $[Al_2O_3H]^+$ and a radical [Eq. (5)]. In an additional pathway, double hydrogen abstrac-

$$[Al_2O_3]^{\bullet+} + NH_3 \rightarrow [Al_2O_3H]^+ + NH_2^{\bullet} \quad (5)$$

tion leading to $[Al_2O_3H_2]^{\bullet+}$ and nitrene is observed [Eq. (6)].

$$[Al_2O_3]^{\bullet+} + NH_3 \rightarrow [Al_2O_3H_2]^{\bullet+} + NH^{\cdot\cdot} \quad (6)$$

The nitrene is of particular interest, as $NH^{\cdot\cdot}$ can react at room temperature with hydrocarbons, such as ethylene, under C–N coupling.[16] That $[Al_2O_3H_2]^{\bullet+}$ is formed in a primary reaction is not only indicated by the slope of the time dependency of the formation of $[Al_2O_3H_2]^{\bullet+}$ (Figure 1c), but also validated by double-resonance experiments[17] of $[Al_2O_3H]^+$ in which the production of $[Al_2O_3H_2]^{\bullet+}$ is not affected when $[Al_2O_3H]^+$ is continuously ejected. Both processes take place with a branching ratio of about 1:1 and they are confirmed by labeling experiments with ND_3. As a result of facile H/D exchange with background water, H-containing product ions are detected as well (see Figure 1b). The rate constant $k([Al_2O_3]^{\bullet+} + NH_3)$ is 3.4×10^{-10} cm^3 s^{-1} molecule^{-1} with ±30% uncertainty; this corresponds to an efficiency of 19%, relative to the gas kinetic collision limit.[18]

DFT calculations were performed to obtain mechanistic insight into the details of the bond-activation processes according to Equations (5) and (6). As already described,[11b] the global minimum of $[Al_2O_3]^{\bullet+}$ corresponds to a four-membered, planar Al-O-Al-O ring with one of the Al atoms (denoted as Al(1)) bearing a terminal oxygen atom (Figure 2a). Geometry optimization of the $[Al_2O_3]^{\bullet+}/NH_3$ encoun-

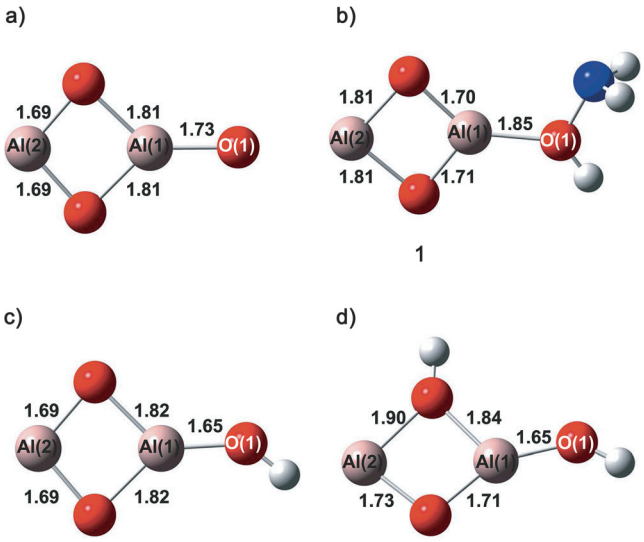

Figure 2. Calculated Al–O bond lengths [Å] for a) $[Al_2O_3]^{\bullet+}$, b) [Al-(μ-O)$_2$-Al(HONH$_2$)]$^{\bullet+}$ (**1**), c) $[Al_2O_3H]^+$, and d) $[Al_2O_3H_2]^{\bullet+}$. For the sake of clarity, charges are omitted. Al ●, O ●, N ●, H ○.

ter complex with coordination of NH_3 to the terminal oxygen atom (denoted as O(1)) leads directly and barrier-free to the formation of the hydroxylamine complex [Al-(μ-O)$_2$-Al-(HONH$_2$)]$^{\bullet+}$ (**1**; Figure 2b), by insertion of O(1) into one of the N–H bonds; this step is exothermic by −146.5 kJ mol^{-1} relative to the separated reactants. In proceeding from $[Al_2O_3]^{\bullet+}/NH_3$ to **1** the (Mulliken) spin density is almost completely transferred from O(1) (1.00) to Al(2) (0.84), that is, the formal oxidation state of Al(2) is reduced from Al^{III} to Al^{II}, and the Al(2)–O bond lengths are increased by 0.12 Å. As was found for the $[Al_2O_3]^{\bullet+}/CH_4$ system,[11b] no radical complex (in this case: $[Al_2O_3H]^+(NH_2^{\bullet})$) can be located on the potential-energy surface (PES) as a minimum.

From intermediate **1**, formation of the product couple $[Al_2O_3H]^+/NH_2^{\bullet}$ is thermodynamically feasible by cleavage of the O(1)–N bond; the reaction in Equation (5) is exothermic by −93.4 kJ mol^{-1}. In contrast, complete oxygen-atom transfer to NH_3 to produce $[Al_2O_2]^{\bullet+}/NH_2OH$ or $Al_2O_2/[NH_2OH]^{\bullet+}$ are endothermic by 89.4 kJ mol^{-1} and 163.7 kJ mol^{-1}, respectively. Further, [Al-(μ-O)$_2$-Al-OH]$^+$, bearing a terminal hydroxy group (Figure 2c), is the only ionic product which is energetically accessible under the experimental conditions. The formation of other conceivable isomers, that is, [Al-(μ-OH)(μ-O)-Al-O]$^+$ or [H-Al-(μ-O)$_2$-Al-O]$^+$, are endothermic by 145.0 kJ mol^{-1} and 360.5 kJ mol^{-1}, respectively. The elimination of $NH_2^{\bullet}$ to generate $[Al_2O_3H]^+$ corresponds to an oxidation of the Al-O-Al-O ring, or more precisely of Al(2). As found for the $[Al_2O_3]^{\bullet+}$ ion, both Al atoms in $[Al_2O_3H]^+$ have formal oxidation states of +3; accordingly, the Al–O

bond lengths within the ring are similar to those calculated for $[Al_2O_3]^{\bullet+}$.

An initial HAT is further possible by the formation of the Lewis acid/base complexes **2** and **5** (Figure 3); moreover, these intermediates serve as the starting points for the second reaction channel found experimentally, that is, double hydrogen-atom transfer. Complex **5** is more stable than **2** by 129.6 kJ mol^{-1}; $TS_{2/5}$ for the intramolecular isomerization **2**⇄**5** (not shown) is located 29.0 kJ mol^{-1} below the separated $[Al_2O_3]^{\bullet+}/NH_3$ reactant pair.

The formation of intermediate **2**, generated by coordination of NH_3 to the sterically less-accessible aluminum atom, Al(1), is exothermic by −223.0 kJ mol^{-1} (Figure 3, top). Starting from **2**, two alternative routes are accessible, that is, the first hydrogen atom can either be transferred to the terminal oxygen O(1) (PES in Figure 3, top, given in blue) or to one of the two bridging oxygen atoms (PES given in red). The barrier associated with the hydrogen transfer to O(1), $TS_{2/3}$, is energetically lower, by 55.0 kJ mol^{-1}, than the barrier $TS_{2/3a}$ leading to the μ-hydroxo species **3a**. This trend continues for the two isomeric species of $[Al_2O_2(OH)(NH_2)]^{\bullet+}$, with **3** being 99.8 kJ mol^{-1} more stable as compared to **3a**.

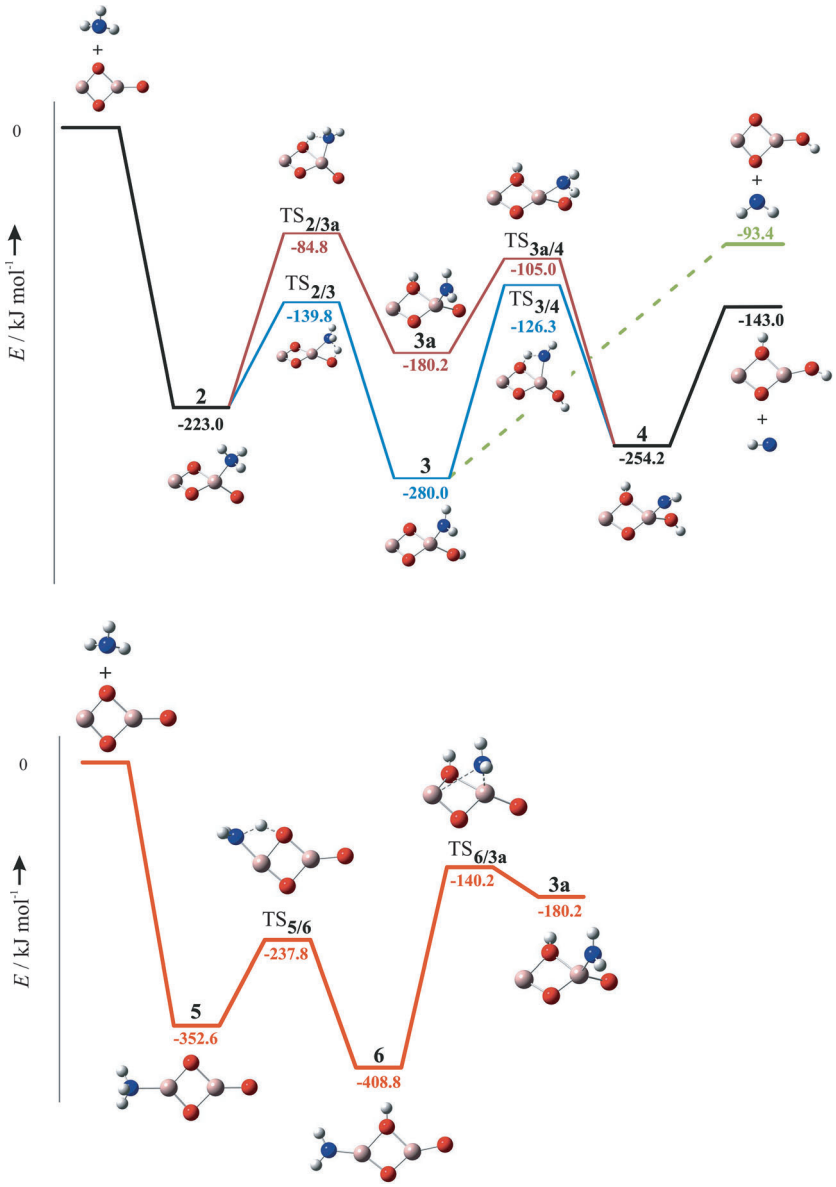

Figure 3. Potential-energy surfaces for the reactions of the $[Al_2O_3]^{\bullet+}/NH_3$ couple via **2** (top) and **5** (bottom). Energies [kJ mol^{-1}]. For the sake of clarity, charges are omitted. Al ●, O ●, N ●, H ○.

Also the transition states associated with the second HAT leading to [Al-(μ-OH)(μ-O)-Al(OH)(NH)]$^{\bullet+}$ (**4**) differ, that is, $TS_{3/4}$ is lower in energy than $TS_{3a/4}$ by 21.3 kJ mol^{-1}. Structure **4** is a common intermediate for both pathways and gives rise to $[Al_2O_3H_2]^{\bullet+}$ by liberation of nitrene in its triplet ground state; the formation of singlet NH is, in line with literature data, energetically much less favored. The most stable structure of $[Al_2O_3H_2]^{\bullet+}$ is given in Figure 2d and corresponds to [Al-(μ-OH)-(μ-O)-Al-OH]$^{\bullet+}$; the formation of other conceivable isomers of $[Al_2O_3H_2]^{\bullet+}$ is endothermic, that is, [H-Al-(μ-O)$_2$-Al-OH]$^{\bullet+}$ (7.4 kJ mol^{-1}), [H-Al-(μ-OH)(μ-O)-Al-O]$^{\bullet+}$ (53.8 kJ mol^{-1}), and [Al-(μ-OH)$_2$-Al-O]$^{\bullet+}$ (111.8 kJ mol^{-1}) and therefore not accessible under thermal conditions. As observed for **1**, the spin density in $[Al_2O_3H_2]^{\bullet+}$ is mainly located on Al(2) (0.89); again, the reduction of Al(2) from the formal oxidation state Al^{III} to Al^{II} is associated with a lengthening of the Al(2)–O bonds (Figure 2d), as already mentioned for the first reaction step $[Al_2O_3]^{\bullet+} + NH_3 \rightarrow$ **1**.

As outlined before, NH_3 can also coordinate to the empty orbital of Al(2) leading to the Lewis acid/base complex **5**; this process is exothermic by −352.6 kJ mol^{-1} (Figure 3, bottom). Next, a hydrogen atom is transferred to a bridging oxygen atom ($TS_{5/6}$), forming the μ-hydroxo species **6** which can isomerize by an intramolecular NH_2 transfer from Al(2) to Al(1) via $TS_{6/3a}$ to form complex **3a**. The formation of **3a** via $TS_{5/6}$ and $TS_{6/3a}$ is energetically more favored than the route **2**→$TS_{2/3a}$→**3a**, because the associated transition structures are by at least 55.4 kJ mol^{-1} lower in energy.

Despite the direct formation of $[Al_2O_3H]^+$ via $[Al_2O_2(HONH_2)]^{\bullet+}$ (**1**), $[Al_2O_3H]^+$ can also be formed by elimination of $NH_2^{\bullet}$ from intermediate **3** (Figure 3, top). However, in this case the reaction has to compete with the energetically much-less-demanding transition structure $TS_{3/4}$; in contrast, an alternative pathway for a second N–H bond activation starting from **1** could not be located on the PESs. Comparing

the thermochemistry for the formation of $[Al_2O_3H]^+$ [Eq. (5)] and $[Al_2O_3H_2]^{\bullet+}$ [Eq. (6)], the reaction in Equation (6) is more favored by 49.6 mol^{-1} than the reaction in Equation (5). However, generation of $[Al_2O_3H_2]^{\bullet+}$ is kinetically more demanding; consequently, both thermodynamic and kinetic factors affect the experimentally observed branching ratio of 1:1.

In this combined experimental/computational study, we describe the first example of single and double N–H bond activation of ammonia by a main-group oxo cluster which results directly in the room-temperature generation of nitrene from NH_3 in a primary reaction.[19]

Experimental Section and Computational Details

The reactions were performed with a Spectrospins CMS 47X FT-ICR mass spectrometer equipped with an external ion source as described elsewhere.[20] First, $[Al_2O_7]^{\bullet+}$ was generated by laser ablation of an aluminum target using a Nd:YAG laser operating at 1064 nm in the presence of about 1% O_2 seeded in the carrier gas.[11a] By using a series of potentials and ion lenses, the ions were transferred into the ICR cell, which was positioned in the center of a 7.05 T superconducting magnet. There, $[Al_2O_3]^{\bullet+}$ was generated by collision-induced dissociation of $[Al_2O_7]^+$ using xenon as a buffer gas, $p(Xe) = 7\times10^{-9}$ mbar, with a collision time of 500 ms.[11a] After thermalization by pulses of argon (ca. 2×10^{-6} mbar) and mass selection using the FERETS ion-ejecting method,[21] the reactions of mass-selected $[Al_2O_3]^{\bullet+}$ were studied by introducing NH_3 or ND_3 using leak valves. The experimental second-order rate constants were evaluated assuming the pseudo first-order kinetic approximation after calibration of the measured pressure and acknowledgement of the ion-gauge sensitivities.[22] For the thermalized cluster ions a temperature of 298 K was assumed.[22] To identify or to rule out possible reactive intermediates as precursor ions, the ion–cyclotron double-resonance technique was applied.[17]

Calculations were performed with the Gaussian 09 program package[23] using TZVP basis sets[24] and the unrestricted B3LYP level of theory;[25] this method proved reliable in previous studies of $[(Al_2O_3)_x]^{\bullet+}$ ($x = 1$, 3–5),[11b,13] $[Al_2O_4]^{\bullet+}$,[26] and $[Al_2O_7]^{\bullet+}$.[11a] To verify stationary points and transition states, frequency calculations were performed. All energies (given in kJ mol^{-1}) are corrected for (unscaled) zero-point vibrational energy contributions. Intrinsic reaction coordinate (IRC) calculations were performed to link transition structures with the corresponding minima.[27]

Received: March 26, 2013
Published online: May 15, 2013

Keywords: ammonia · hydrogen abstraction · N–H activation · nitrene · oxide cluster

[1] a) *Comprehensive Natural Products Chemistry, Vol. 4* (Eds.: D. H. R. Barton, K. Nakanishi, O. Meth-Cohn), Elsevier, Oxford, **1999**; b) R. Hili, A. K. Yudin, *Nat. Chem. Biol.* **2006**, *2*, 284–287; c) J. P. Corbet, G. Mignani, *Chem. Rev.* **2006**, *106*, 2651–2710; d) G. Evano, N. Blanchard, M. Toumi, *Chem. Rev.* **2008**, *108*, 3054–3131; e) *Handbook of Heterogeneous Catalysis, 2nd ed.* (Eds.: G. Ertl, H. Knözinger, F. Schüth, J. Weitkamp), Wiley-VCH, Weinheim, **2008**.

[2] M. B. Smith, J. March, *March's Advanced Organic Chemistry: Reactions, Mechanisms, and Structure, 6th ed.*, Wiley, Hoboken, **2007**.

[3] a) P. Müller, C. Fruit, *Chem. Rev.* **2003**, *103*, 2905–2919; b) A. R. Dick, M. S. Sanford, *Tetrahedron* **2006**, *62*, 2439–2463; c) J. I. van der Vlugt, *Chem. Soc. Rev.* **2010**, *39*, 2302–2322; d) J. L. Klinkenberg, J. F. Hartwig, *Angew. Chem.* **2011**, *123*, 88–98; *Angew. Chem. Int. Ed.* **2011**, *50*, 86–95.

[4] T. Braun, *Angew. Chem.* **2005**, *117*, 5138–5140; *Angew. Chem. Int. Ed.* **2005**, *44*, 5012–5014.

[5] a) K. Eller, H. Schwarz, *Chem. Rev.* **1991**, *91*, 1121–1177; b) A. A. Viggiano, S. T. Arnold, R. A. Morris, *Int. Rev. Phys. Chem.* **1998**, *17*, 147–184; c) D. K. Böhme, H. Schwarz, *Angew. Chem.* **2005**, *117*, 2388–2406; *Angew. Chem. Int. Ed.* **2005**, *44*, 2336–2354; d) D. K. Böhme, *Can. J. Chem.* **2008**, *86*, 177–198.

[6] a) J. Roithová, D. Schröder, *Chem. Rev.* **2010**, *110*, 1170–1211; b) H. Schwarz, *Angew. Chem.* **2011**, *123*, 10276–10297; *Angew. Chem. Int. Ed.* **2011**, *50*, 10096–10115; c) N. Dietl, M. Schlangen, H. Schwarz, *Angew. Chem.* **2012**, *124*, 5638–5650; *Angew. Chem. Int. Ed.* **2012**, *51*, 5544–5555.

[7] a) M. Ončák, Y. L. Cao, R. F. Höckendorf, M. K. Beyer, R. Zahradník, H. Schwarz, *Chem. Eur. J.* **2009**, *15*, 8465–8474; b) G. K. Koyanagi, V. Kapishon, D. K. Böhme, X. Zhang, H. Schwarz, *Eur. J. Inorg. Chem.* **2010**, 1516–1521; c) G. K. Koyanagi, P. Cheng, D. K. Böhme, *J. Phys. Chem. A* **2010**, *114*, 241–246; d) R. Kretschmer, X. H. Zhang, M. Schlangen, H. Schwarz, *Chem. Eur. J.* **2011**, *17*, 3886–3892; e) R. Kretschmer, M. Schlangen, H. Schwarz, *Chem. Eur. J.* **2012**, *18*, 40–49; f) R. Kretschmer, M. Schlangen, H. Schwarz, *Chem. Asian J.* **2012**, *7*, 1214–1220.

[8] D. Schröder, H. Schwarz, *Angew. Chem.* **1995**, *107*, 2126–2150; *Angew. Chem. Int. Ed. Engl.* **1995**, *34*, 1973–1995.

[9] a) S. W. Buckner, B. S. Freiser, *J. Am. Chem. Soc.* **1987**, *109*, 4715–4716; b) S. W. Buckner, J. R. Gord, B. S. Freiser, *J. Am. Chem. Soc.* **1988**, *110*, 6606–6612; c) K. K. Irikura, J. L. Beauchamp, *J. Am. Chem. Soc.* **1989**, *111*, 75–85; d) E. F. Fialko, A. V. Kikhtenko, V. B. Goncharov, K. I. Zamaraev, *J. Phys. Chem. A* **1997**, *101*, 8607–8613; e) M. Brönstrup, D. Schröder, H. Schwarz, *Chem. Eur. J.* **1999**, *5*, 1176–1185; f) B. Chiavarino, M. E. Crestoni, S. Fornarini, *Chem. Eur. J.* **2002**, *8*, 2740–2746; g) S. Hirabayashi, M. Ichihashi, T. Kondow, *J. Phys. Chem. A* **2010**, *114*, 13040–13044.

[10] S. Heinbuch, F. Dong, J. J. Rocca, E. R. Bernstein, *J. Chem. Phys.* **2010**, *133*, 1743141–17431411.

[11] a) Z.-C. Wang, T. Weiske, R. Kretschmer, M. Schlangen, M. Kaupp, H. Schwarz, *J. Am. Chem. Soc.* **2011**, *133*, 16930–16937; b) Z.-C. Wang, N. Dietl, R. Kretschmer, J.-B. Ma, T. Weiske, M. Schlangen, H. Schwarz, *Angew. Chem.* **2012**, *124*, 3763–3767; *Angew. Chem. Int. Ed.* **2012**, *51*, 3703–3707.

[12] M. Trueba, S. P. Trasatti, *Eur. J. Inorg. Chem.* **2005**, 3393–3403.

[13] S. Feyel, J. Döbler, R. Hoeckendorf, M. K. Beyer, J. Sauer, H. Schwarz, *Angew. Chem.* **2008**, *120*, 1972–1976; *Angew. Chem. Int. Ed.* **2008**, *47*, 1946–1950.

[14] H. Muroyama, C. Saburi, T. Matsui, K. Eguchi, *Appl. Catal. A* **2012**, *443*, 119–124.

[15] a) M. Ni, M. K. H. Leung, D. Y. C. Leung, *Int. J. Energy Res.* **2009**, *33*, 943–959; b) F. Schüth, R. Palkovits, R. Schlögl, D. S. Su, *Energy Environ. Sci.* **2012**, *5*, 6278–6289.

[16] A. F. Holleman, E. Wiberg, *Lehrbuch der Anorganischen Chemie, 101th ed.*, Walter de Gruyter, Berlin, New York, **1995**.

[17] M. B. Comisarow, V. Grassi, G. Parisod, *Chem. Phys. Lett.* **1978**, *57*, 413–416.

[18] Collision-rate calculations (G. Gioumousis, D. P. Stevenson, *J. Chem. Phys.* **1958**, *29*, 294–299) were performed by using the ADO method: T. Su, M. T. Bowers, *J. Chem. Phys.* **1973**, *58*, 3027–3037.

[19] For recent articles on multiple C–H bond activation by metal oxide clusters, see a) G. de Petris, A. Cartoni, A. Troiani, V. Barone, P. Cimino, G. Angelini, O. Ursini, *Chem. Eur. J.* **2010**, *16*, 6234–6242; b) X.-N. Wu, X.-N. Li, X.-L. Ding, S.-G. He, *Angew.*

Chem. **2013**, *125*, 2504 – 2508; *Angew. Chem. Int. Ed.* **2013**, *52*, 2444 – 2448; c) N. Dietl, X. Zhang, C. van der Linde, M. K. Beyer, M. Schlangen, H. Schwarz, *Chem. Eur. J.* **2013**, *19*, 3017 – 3028; d) Z.-C. Wang, S. Yin, E. R. Bernstein, *J. Phys. Chem. A* **2013**, *117*, 2294 – 2301, and references therein.

[20] a) K. Eller, H. Schwarz, *Int. J. Mass Spectrom. Ion Processes* **1989**, *93*, 243 – 257; b) K. Eller, W. Zummack, H. Schwarz, *J. Am. Chem. Soc.* **1990**, *112*, 621 – 627.

[21] R. A. Forbes, F. H. Laukien, J. Wronka, *Int. J. Mass Spectrom. Ion Processes* **1988**, *83*, 23 – 44.

[22] D. Schröder, H. Schwarz, D. E. Clemmer, Y. Chen, P. B. Armentrout, V. I. Baranov, D. K. Böhme, *Int. J. Mass. Spectrom. Ion Processes* **1997**, *161*, 175 – 191.

[23] Gaussian 09 (Revision A.1), M. J. Frisch, G. W. Trucks, H. B. Schlegel, G. E. Scuseria, M. A. Robb, J. R. Cheeseman, G. Scalmani, V. Barone, B. Mennucci, G. A. Petersson, H. Nakatsuji, M. Caricato, X. Li, H. P. Hratchian, A. F. Izmaylov, J. Bloino, G. Zheng, J. L. Sonnenberg, M. Hada, M. Ehara, K. Toyota, R. Fukuda, J. Hasegawa, M. Ishida, T. Nakajima, Y. Honda, O. Kitao, H. Nakai, T. Vreven, J. A. Montgomery, J. E. Peralta, F. Ogliaro, M. Bearpark, J. J. Heyd, E. Brothers, K. N. Kudin, V. N. Staroverov, R. Kobayashi, J. Normand, K. Raghavachari, A. Rendell, J. C. Burant, S. S. Iyengar, J. Tomasi, M. Cossi, N. Rega, N. J. Millam, M. Klene, J. E. Knox, J. B. Cross, V. Bakken, C. Adamo, J. Jaramillo, R. Gomperts, R. E. Stratmann, O. Yazyev, A. J. Austin, R. Cammi, C. Pomelli, J. W. Ochterski, R. L. Martin, K. Morokuma, V. G. Zakrzewski, G. A. Voth, P. Salvador, J. J. Dannenberg, S. Dapprich, A. D. Daniels, Ö. Farkas, J. B. Foresman, J. V. Ortiz, J. Cioslowski, D. J. Fox, Gaussian Inc. Wallingford CT, **2009**.

[24] A. Schäfer, C. Huber, R. Ahlrichs, *J. Chem. Phys.* **1994**, *100*, 5829 – 5835.

[25] a) C. Lee, W. Yang, R. G. Parr, *Phys. Rev. B* **1988**, *37*, 785 – 789; b) A. D. Becke, *J. Chem. Phys.* **1993**, *98*, 5648 – 5652.

[26] Z. C. Wang, X. N. Wu, Y. X. Zhao, J. B. Ma, X. L. Ding, S. G. He, *Chem. Phys. Lett.* **2010**, *489*, 25 – 29.

[27] a) K. Fukui, *J. Phys. Chem.* **1970**, *74*, 4161 – 4163; b) K. Fukui, *Acc. Chem. Res.* **1981**, *14*, 363 – 368; c) C. Gonzalez, H. B. Schlegel, *J. Phys. Chem.* **1990**, *94*, 5523 – 5527; d) D. G. Truhlar, M. S. Gordon, *Science* **1990**, *249*, 491 – 498.

